Longitudinal Elastic Velocities in MgO to 360 kbar

LYLE D. MEIER AND THOMAS J. AHRENS

Seismological Laboratory, California Institute of Technology, Pasadena, California 91125

Numerical descriptions of shock wave induced flows obtained with a two-dimensional Lagrangian finite difference code are compared in detail with experimental data obtained via the lateral relaxation method for polycrystalline magnesium oxide (MgO) to a pressure of 360 kbar. The equation of state used for MgO was assumed to be of the Mie-Grüneisen form, and detailed comparison of experimental and calculated data was used to obtain refined values of the shear strength and shear modulus of MgO at high pressures. The best fitting rheological model for MgO was characterized by a shear strength which decreased from a value of 26 kbar at 16.5-kbar mean stress to 13.5 kbar at 360-kbar mean stress along the principal Hugoniot curve. The first and second pressure derivatives of the shear modulus, when the shear modulus is evaluated as a quadratic function of pressure, yield $(\partial\mu/\partial P) = 2.44$ and $\mu(\partial^2\mu/\partial P^2) = 1.7 \pm 3.0$. The uncertainties in the determination of $\mu(\partial^2\mu/\partial P^2)$ have been reduced by a factor of 5 over previous estimates.

INTRODUCTION

In order to better understand the internal constitution of the earth it is important to obtain knowledge of the behavior of elastic moduli of minerals at pressures and temperatures appropriate to the interior. To date, shock wave experiments have yielded considerable information about the relationship between pressure and density, and hence about bulk modulus, for a considerable number of silicates, oxides, and metallic minerals. In order to more fully examine possible constituents of the earth's interior it is desirable to obtain information about the pressure dependence of the shear modulus to very high pressures. Finite strain extrapolations of elastic constants, measured at relatively low pressures, provide a means of estimating shear moduli to large compressions. Since the data set upon which these extrapolations are based usually provides only the first pressure derivative of the elastic moduli, at pressures less than 10 kbar, direct measurements of shear moduli at high pressures are desirable [*Davies and Ahrens*, 1973; *Birch*, 1952; *Thomsen*, 1970, 1972]. For magnesium oxide, a mineral of importance in many models of the lower mantle, elastic parameters have been measured ultrasonically to 3 kbar and 473°K by *O. L. Anderson et al.* [1968] and *Chung* [1963] and reported over the range 0–10 kbar and 300°–1000°K by *Spetzler* [1970] and *Spetzler and Anderson* [1971].

Two optical methods have been suggested for determining the shear elastic moduli of materials at very high shock pressures [*Al'tschuler et al.*, 1960; *Fowles*, 1960]. In addition, in-material gages [*Al'tschuler et al.*, 1967; *Grady et al.*, 1975] have been used to measure release wave velocities. The optical methods involve measurement of the velocity of propagation of release waves into shocked portions of the sample. *Al'tschuler et al.* [1960] report measurements of the isentropic compressional wave velocity as release waves propagate into metals shocked to high pressures. The first of these methods, termed the 'overtaking relaxation method' by *Al'tschuler et al.* [1960], is used to obtain the velocity of release waves by observing the point on a wedge-shaped sample where release waves from the rear surface of the flyer plate, after propagation through the wedge, overtake the shock emanating from the surface of collision between the sample and the flyer plate. This method was used by *Bless and Ahrens* [1976] to measure elastic moduli of aluminum oxide. The other method, termed the 'lateral relaxation method' by *Al'tschuler et al.* [1960], measures the velocity of release waves propagating toward the center of a cylindrical or cubic sample from the edges. This method has been applied by *Van Thiel et al.* [1974] to study the properties of deuterium and by *Davies and Ahrens* [1973] to the measurement of the elastic moduli of magnesium oxide at very high pressures. This study was undertaken to obtain more information from Davies and Ahrens's experiment through application of numerical simulation, and it sought to find the elastic and strength parameters which best fit their complete lateral relaxation profile.

METHOD

The experimental geometry used by *Davies and Ahrens* [1973] and used in the present numerical simulation is shown in Figure 1. A flyer plate of tungsten is accelerated to a velocity of 1.6 km/s by a high-performance powder gun. This flyer plate impacts a driver plate also made of tungsten. On this driver plate a polycrystalline sample of MgO is mounted. A mirror is placed a short distance above the upper surface of the MgO and is observed with a streak camera, which records the reflectivity of the mirror versus time. The impact of the flyer plate into the driver plate creates a flat-topped shock wave with an amplitude in the tungsten of 740 kbar. As this shock wave propagates into the MgO, the amplitude of the shock wave decreases to 360 kbar, owing to the impedance mismatch between tungsten and MgO. As the shock wave propagates into the sample, which is shaped as shown in Figure 1, a release (or edge) wave propagates into the center of the specimen. As this wave propagates, the velocity of mass elements along the sides of the MgO is directed away from the center of the sample, and thus the pressure is reduced there. If the material is assumed to behave according to the elastic plastic model of *Fowles* [1961], the release wave will have two phases. The first is an elastic phase, traveling at the local compressional wave velocity $[(K_s + \frac{4}{3}\mu)/\rho]^{1/2}$ (where K_s and μ are the isentropic bulk and shear moduli and ρ is density) in the high-pressure shocked region with an amplitude determined, in principle, by the maximum shear stress supportable by the material. This phase releases the one-dimensional elastic stress in the body. The second phase of the release wave travels at the local dynamic bulk wave speed $(K_s/\rho)^{1/2}$ behind the first phase of the release wave. This wave presumably releases hydrostatic stress in the material to some lower pressure. In *Davies and*

Paper number 7B0062.

Ahrens's [1973] experiment a mirror–free surface separation was utilized in order to eliminate the effects of the elastic precursor to the shock wave. As the shock wave reaches the upper free surface of the sample, the central portion of the shock wave is unaffected by the lateral surfaces, resulting in high and uniform free surface velocity. The shock wave near the edges of the sample has been attenuated owing to the presence of the release wave, resulting in both a later arrival of the shock wave at the free surface and a smaller amplitude of the arriving shock wave. The weaker shock wave produces a lower value for the free surface velocity than the unattenuated shock wave. This free surface velocity difference results in the central portion of the free surface reaching the mirror before the peripheral portions of the free surface. Thus the free surface takes progressively longer to reach the mirror the nearer it is to the edge of the sample. Davies and Ahrens determine the apparent release wave velocity by noting the limits on the streak record of the region affected by the release wave. This is taken to be the point at which the slope of the reflectivity versus time profile changes. Noting this point, one obtains, using Figure 1, an expression for the release wave velocity V_r [see *Al'tschuler et al.*, 1960]:

$$V_r = U_s\{(\tan \alpha)^2 + [(U_s - U_p)/U_s]^2\}^{1/2} \quad (1)$$

U_s is the shock velocity, U_p is the particle velocity behind the unattenuated shock, and α is the angle defined in Figure 1. A difficulty with this method is the uncertainty associated with picking the limit of influence of the release wave. In addition, the free surface profile of the sample may change during the travel time of the free surface to the mirror.

NUMERICAL METHOD

A series of two-dimensional impact-induced flows were simulated by utilizing the TOODY-IIA Lagrangian finite difference code of *Bertholf and Benzley* [1968]. A Cartesian geometry was used for the calculations in preference to a cylindrical geometry, since the sample is shaped as is shown in Figure 1. The edge effect, or release wave, only perturbs the outer portions of the reflectivity profile and thus is more appropriately simulated with a Cartesian geometry. The release wave travels a distance approximately equal to the distance from the center of the mirror to the start of the curved portion of the sample. This results in the effects due to the curved sides of the sample not affecting the release wave in any significant manner, thus justifying the use of a Cartesian geometry.

The equations of state for the magnesium oxide and the tungsten were assumed to be of the Mie-Grüneisen form, with a reference state chosen to lie along the Hugoniot. We assume a linear shock velocity–particle velocity relationship:

$$U_s = C_0 + SU_P \quad (2)$$

Here C_0 is the zero-pressure bulk wave speed, and S is given by the

$$S = (K_{s0}' + 1)/4 \quad (3)$$

where K_{s0}' is the first pressure derivative of the isentropic bulk modulus at zero pressure [*Ruoff*, 1967]. Let R be the volumetric strain in the material. Then,

$$R = 1 - (\rho/\rho_0) \quad (4)$$

Here ρ_0 is the zero-pressure value of the density. Combining (2) and (4) and the Rankine-Hugoniot equations yields

$$\sigma_h = \rho_0 C_0^2 R/(1 - SR)^2 \quad (5)$$

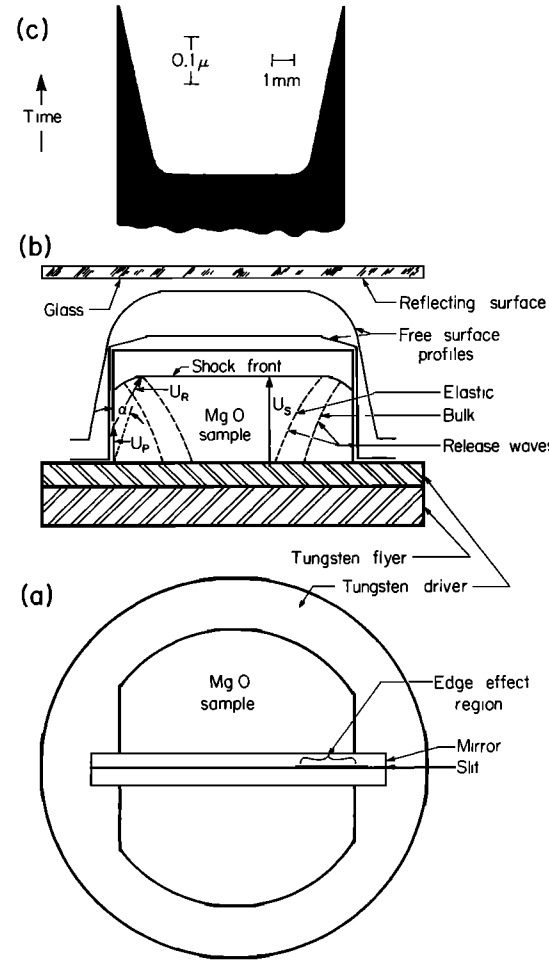

Fig. 1. Geometry of flow resulting from impact and its relationship to experimental observations. (*a*) Top view of sample. Lateral release wave propagates inward and hence is simulated by Cartesian motion. (*b*) Side view of experiment. Two-wave structure of the release wave is shown along with profiles of sample at two times after impact. (*c*) Hypothetical streak camera record of mirror reflectivity resulting from impact.

where σ_h is the one-dimensional stress along the Hugoniot. For states not along the Hugoniot the Mie-Grüneisen equation is then used to obtain the appropriate mean principal stress P_m at the energy present in the cell. For an elastoplastic rheology,

$$P_m = \Gamma\rho(E_d - E_h) + P_h \quad (6)$$

where E_d is the energy in the mass element being studied, E_h is the energy along the Hugoniot, appropriate to P_h, and Γ is the Grüneisen's parameter for the sample. The stress components (positive in compression) are determined as follows:

$$d\tau_{\alpha\beta} = \tau_{\alpha\beta} - \delta_{\alpha\beta}P_m \quad (7)$$

where the $\tau_{\alpha\beta}$ are the components for the two-dimensional Cartesian stress tensor, $d\tau_{\alpha\beta}$ are the deviatoric, or nonhydrostatic, portions of the stress, and α and β may be either x or z. The deviatoric stress components are determined by using elasticity relations. If this stress state violates the Von Mises yield criterion [*Bridgman*, 1952],

$$[(d\tau_{xx})^2 + (d\tau_{zz})^2 + (d\tau_{xz})^2 + (d\tau_{xx})(d\tau_{zz})] \leq \tfrac{2}{3}Y^2 \quad (8)$$

where Y is the yield surface stress state, the stress states are corrected so that they lie on the yield surface. The pressure

TABLE 1. Parameters of Equation of State for MgO and Tungsten

Property	Tungsten	MgO
ρ_0, g/cm^3	19.22	3.58
K_0, 10^3 kbar	3.1	1.62
S	1.23	1.35
ν	0.25	0.18
Γ	1.54	1.52

derivative of the bulk modulus is determined from (5) and (6) by taking appropriate derivatives. The temperature derivative is determined by calculating the expansion of the specimen with temperature at room pressure and using the density thus obtained to calculate the bulk modulus.

The shear modulus was specified either as a constant multiple of bulk modulus (cases 3 and 6; see Table 3 for explanation of cases) or by assuming pressure derivatives to be input parameters (cases 4 and 5) and the temperature derivatives to be zero for computational simplicity. (Since the maximum temperature reached in the shock is only about 500°K, the effect of this assumption is to make the shear modulus about 10% too large at zero pressure.) Table 1 lists the parameters used to specify the equations of state of tungsten and MgO. Table 2 lists the values of the temperature and pressure derivatives of the bulk modulus for MgO and compares these values with experimentally measured values. The calculated values lie within the range of values measured experimentally, and the temperature derivatives are shown for the purpose of indicating the results of applying simple Mie-Grüneisen theory.

RESULTS

A series of calculations were conducted by utilizing the matrix of parameters listed in Table 3. By using the calculations to obtain V_r via (1) for case 4 the release wave velocity is determined by the method of *Davies and Ahrens* [1973] and listed in Table 4. This demonstrates an apparent release wave velocity increase with increasing mirror–free surface distance. The theoretical calculations give a very low amplitude arrival at an apparent release wave velocity of 10.5 ± 1 km/s on the synthetic streak record with the smallest mirror–free surface distance (0.005 cm). This is the predicted velocity for longitudinal compressional waves for the equation of state assumed, thus indicating the agreement of the calculations with expected values. This arrival is of such low magnitude (Figure 2) that it would not be experimentally detectable. The arrival is not seen in calculated profiles for larger mirror–free surface distances, owing to distortion of the free surface during the time interval required for it to traverse the distance between its initial position and that of the mirror. Table 4 demonstrates that the apparent release wave velocity which would be experimentally inferred increases from values of approximately those of the bulk sound speed at small mirror–free surface distances without bound to a value above both that obtained by *Davies and Ahrens* [1973] for the longitudinal sound speed in the material and that predicted by the equation-of-state model. The increasing distortion of the free surface with time is reflected in the calculated mirror impact profiles of Figure 3. Examination of the profiles in the figure shows changes in the shape and sharpness of the transition region with increasing mirror–free surface distance. This result confirms Davies and Ahrens's suggestion that this effect is a major source of error in applying (1).

Utilizing the matrix outlined in Table 3, we attempted to find a model for the equation of state of MgO which best fit the experimental data from shot A-257. This shot was selected because of the superior photographic quality of the data and the small mirror–free surface separation used in the shot. The small value of mirror–free surface separation was chosen in order to minimize the numerical roundoff errors in the calculation. Figure 4 shows the results of comparing the calculated and observed mirror impact times for several different cases. The estimated error in comparing the calculated and experimental profiles is about 0.015 μs and results from the finite width of the transition between the reflecting and nonreflecting portions of the record. Figure 4 demonstrates that this method is markedly sensitive to differences in the first pressure derivative of the shear modulus and is also sensitive to changes in the maximum shear stress supportable by the material. The results of this figure may also indicate sensitivity to the second pressure derivative of the shear modulus. The trend displayed for cases 3, 4, and 5 indicates that the best value of the first pressure derivative of the shear modulus, evaluated at 360 kbar, is nearest to 2.87. Case 6 indicates that the best model for the maximum shear stress has the maximum shear stress supportable by MgO decreasing linearly from 26.0 kbar at 16.5-kbar mean stress to 13.5 kbar at 360-kbar mean stress, with the yield surface being given by

$$Y = 27.0 - 0.0375P_m \quad \text{kbar} \tag{9}$$

DISCUSSION

The results for the varying yield strength in MgO may be explained in several ways. One possibility is that as the temperature of the specimen increases owing to the passage of the shock wave, the (100) ⟨110⟩ slip system may be activated, resulting in lower material strength as suggested by *Paterson and Weaver* [1970]. Alternatively, the actual shear strength of the material may decrease. For MgO, *Kinsland and Bassett* [1976] report that the yield strength increases to a maximum of 30 kbar at about 50-kbar mean stress and then remains effectively constant to ~250 kbar, although there is considerable scatter in the low-pressure Kinsland and Bassett data (the shear strength is of the same magnitude as that obtained by *Bridgman* [1937] in his early semiquantitative study). However, their data do not preclude a gradual decrease in Y, which we infer. For reference, we show (9) in relation to their data obtained from ellipticities of the (200) reflection (Figure 5). Note that *Dandekar* [1976] has recently observed an apparent decrease in shear strength with increasing shock pressure in tungsten. He suggests that an elastic isotropic equation of state may be an appropriate shock rheology for this material. *Ahrens* [1966] has reported values of the Hugoniot elastic limit for MgO ranging from 34.5 to 89 kbar. The value of shear strength used here is appropriate to a Hugoniot elastic limit of 34.5 kbar, where the Hugoniot elastic limit σ_{hel} is related to the yield strength Y by

TABLE 2. Comparison of Calculated and Experimental Values of Isotropic Elastic Constants of MgO

Property	Calculated	Experimental
K_0, 10^3 kbar	1.626	1.624
$(\partial K/\partial P)_{P=0}$	3.8	4.50
$(\partial K_s/\partial T)_{T=300°K}$, kbar/°K	−0.166	−0.15
$(\partial \mu/\partial T)_{T=300°K}$, kbar/°K	−0.153	−0.25

Data are from *Spetzler* [1971] and *O. L. Anderson et al.* [1968].

TABLE 3. Values of Variable Parameters Used in the Calculation

Case	Case Number	$(\partial\mu/\partial P)_{P=0}$	$\mu(\partial^2\mu/\partial P^2)$	$V_p(0)$, km/s	V_p(360 kbar), km/s	$Y_{P=0}$	$Y_{P=360\text{kbar}}$
Literature*	0	2.62	-1.0 ± 15	9.75	11.5	13.5	13.5
Hydrostatic	1	3.56	−2.7	6.74	8.42	0.0	0.0
Elastic plastic	3	3.56	−2.7	9.75	11.85	13.5	13.5
Constant shear modulus	4	0.0	0.0	9.75	10.55	13.5	13.5
Low-pressure derivative of shear modulus	5	2.44	0.0	9.75	11.85	13.5	13.5
Variable elastic limit	6	3.56	−2.7	9.75	11.85	27.0	13.5

* Data are from *Spetzler* [1971], *Spetzler and Anderson* [1971], *O. L. Anderson et al.* [1968], *Davies and Ahrens* [1973], and *Ahrens* [1966].

$$\sigma_{hel} = [(1 - \nu)/(1 - 2\nu)]Y \quad (10)$$

where ν is Poisson's ratio.

The value of the first pressure derivative of the shear modulus at 360-kbar mean stress is indicated to be 2.87. Using this value and the ultrasonically measured values of $\partial\mu/\partial P$ at P = 1 bar, we obtain $(\partial\mu/\partial P) = 2.62$ [*O. L. Anderson et al.*, 1968] and $\mu(\partial^2\mu/\partial P^2) = 0.9 \pm 3.0$. If $(\partial\mu/\partial P)_{P=1\text{bar}} = 2.44$, then $\mu(\partial^2\mu/\partial P^2) = 1.7 \pm 3.0$. The latter values of $\partial\mu/\partial P$ and $\mu(\partial^2\mu/\partial P^2)$ are probably the most reliable. The difference between the results of the third-order extrapolation giving V_P = 11.3 km/s (which does not use $\mu(\partial^2\mu/\partial P^2)$ and therefore is unchanged from the value cited by *Davies and Ahrens* [1973]) and the fourth-order value obtained with our value of $\mu(\partial^2\mu/\partial P^2)$ which gives V_P = 11.9 km/s is significant. This difference indicates the importance of using fourth-order finite strain extrapolations of elastic moduli for MgO in the range of volumetric strains from 0.01 (70 kbar) to at least volumetric strains of 0.06 (360 kbar). These values are well within the values reported by *Davies and Ahrens* [1973] of -1.0 ± 15,0, and the uncertainty is significantly reduced. However, the previous limits on $\mu(\partial\mu/\partial P^2)$ provided little bound on the behavior of the shear modulus, since the value of the first derivative at 360-kbar mean stress could vary between +5.94 and −1.66, evidently not a great constraint upon the behavior of the shear modulus.

Using the values listed above for the pressure derivatives of the shear modulus, we obtain a value of the compressional wave velocity in MgO at 360-kbar mean principal stress of 11.9 km/s, as compared with *Davies and Ahrens*'s [1973] value, based upon a fourth-order finite strain extrapolation of 11.5 km/s. Davies and Ahrens's third-order value of the compressional wave speed at the same pressure is 11.3 km/s. (Note that we do not change μ_0 or $\partial\mu/\partial P$; therefore the result of the third-order extrapolation will not change.) These values were obtained through the use of the following basic expressions (simplified from *Davies* [1974]):

$$C_i = (1 + 2\eta)^{1/2}(C_{i0} + C_i'\eta + \tfrac{1}{2}C_i''\eta^2) \quad (11)$$

$$C_i' = 3K_0C_{i0}' - C_{i0} \quad (12)$$

$$C_i'' = 9K_0^2C_{i0}'' - 3K_0'(C_{i0} + C_i') - 4C_i' - C_{i0} \quad (13)$$

Here K_0 is the zero-pressure bulk modulus, and K_0' is the first pressure derivative of the bulk modulus at zero pressure. The C_i are the isotropic elastic moduli (λ, μ), the Lame constants, or the bulk and shear moduli (K, μ); C_{i0} is the zero-pressure value of the modulus; C_{i0}' is the first pressure derivative of the modulus evaluated at zero pressure; C_{i0}'' is the second pressure derivative of the modulus; and

$$\eta = \tfrac{1}{2}[(\rho/\rho_0)^{2/3} - 1] \quad (14)$$

These results imply that the compressional wave velocity of MgO at 360-kbar mean principal stress is about 11.9 km/s and the shear velocity is 7.0 km/s. Previous models of the shear velocity of MgO in the lower mantle have utilized only third-order extrapolations; therefore their predictions of the veloci-

TABLE 4. Apparent Release Wave Velocity Compared With Mirror–Free Surface Separation for Case 4

Mirror–Free Surface Separation, cm	Apparent Release Wave Velocity, km/s
0.005	8.94 ± 0.03*†
0.010	8.99 ± 0.25†
0.015	9.96 ± 0.9†
0.025	10.16 ± 0.82†
0.035	10.95 ± 0.9‡
0.045	10.83 ± 0.6‡
0.050	10.89 ± 0.7‡
0.060	11.37 ± 0.7‡
0.070	11.06 ± 0.6‡
0.080	11.37 ± 0.26
0.090	11.78 ± 0.5‡
0.100	12.36 ± 0.30‡

* Actual longitudinal arrival gives 10.55 km/s (Figure 3).
† Approximate bulk release wave arrival velocity.
‡ Spurious apparent arrivals due to distortion of free surface.

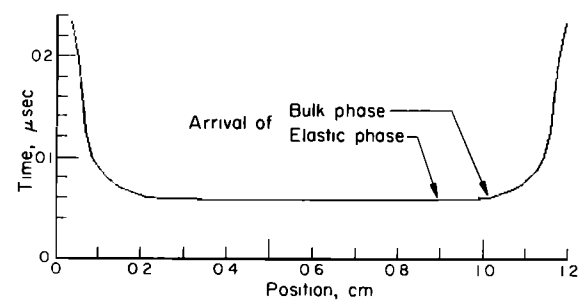

Fig. 2. Calculated profile for case 4, with a mirror-free surface separation of 0.005 cm. The elastic phase of the release wave arrives with an apparent velocity of 10.5 km/s, as predicted by the equation-of-state model for this case, although this arrival is masked by distortion of free surface at larger mirror-free surface distances.

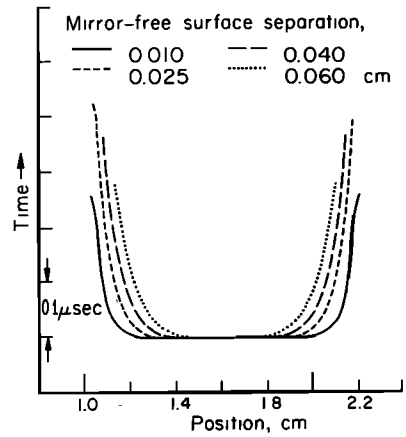

Fig. 3. Calculated mirror reflectivity profiles for various mirror-free surface distances, illustrating changes in the shape of the mirror reflectivity profile with varying mirror-free surface distance.

ties of MgO will be systematically too low [*D. L. Anderson et al.*, 1971]. The higher shear velocity predicted by the results of this paper will tend to reduce the amount of MgO in the lower mantle to allow the shear velocity to match that measured seismically.

Acknowledgments. We wish to thank L. D. Bertholf and his colleagues for kindly providing the TOODY-IIA computer code, R. C. Liebermann, M. S. Paterson, H. C. Heard, and D. L. Anderson for helpful comments on the manuscript, and Geoffrey Davies for discussions during the initiation of this work. This work was supported by National Science Foundation grant DES75-15006. Contribution 2802, Division of Geological and Planetary Sciences, California Institute of Technology, Pasadena, California 91125.

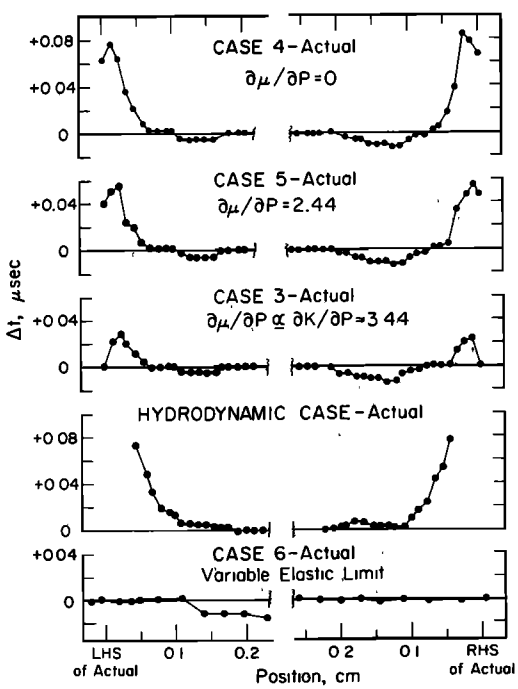

Fig. 4. Time residuals between calculated loss of mirror reflectivity and experimental profiles at various positions. Arrivals in central unattenuated region were constrained to be simultaneous. Note that the central portion of mirror of reflectivity profile time differences is omitted from this plot. Estimated error in determining arrival time differences is 0.015 μs.

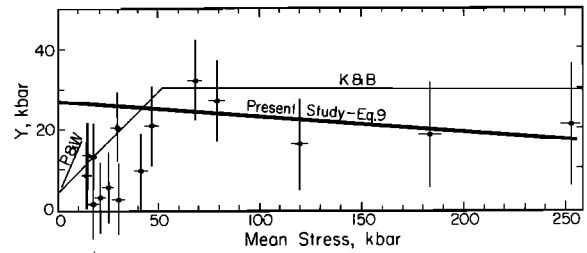

Fig. 5. Comparison of yield strength versus mean stress for MgO. Data reported by *Kinsland and Bassett* [1976] (K&B) using ellipticity of (200) reflection in diamond anvil apparatus is compared with the data inferred from present study (equation (9)). Low-pressure data of *Paterson and Weaver* [1970] (P&W) are also indicated.

REFERENCES

Ahrens, T. J., High pressure electrical behavior and equation of state of magnesium oxide from shock wave measurements, *J. Appl. Phys., 37*, 2532, 1966.

Al'tschuler, L. V., S. B. Kormer, M. I. Brazhnik, M. P. Vladimirov, M. P. Speranskaya, and A. I. Funtikov, The isentropic compressibility of aluminum, copper, lead, and iron at high pressure, *Sov. Phys. JETP*, Engl. Transl., *11*, 766, 1960.

Al'tschuler, L. V., M. N. Pavlovskii, and V. P. Drakin, Peculiarities of phase transitions in compression and rarefaction shock waves, *Sov. Phys. JETP*, Engl. Transl., *25*, 260, 1967.

Anderson, D. L., C. Sammis, and T. Jordan, Composition and evolution of the mantle and core, *Science, 171*, 1103, 1971.

Anderson, O. L., E. Schreiber, R. C. Liebermann, and N. Soga, Some elastic constant data on minerals relevant to geophysics, *Rev. Geophys. Space Phys., 6*, 491, 1968.

Bertholf, L. D., and S. E. Benzley, TOODY IIA: A computer program for two dimensional wave propagation, *Rep. SC-RR-68-41*, Sandia Lab., Albuquerque, N. Mex., 1968.

Birch, F., Elasticity and constitution of the earth's interior, *J. Geophys. Res., 57*, 227, 1952.

Bless, S., and T. J. Ahrens, Measurement of release wave speed in shock compressed polycrystalline alumina and aluminum, *J. Geophys. Res., 81*, 1935, 1976.

Bridgman, P. W., Shearing phenomena at high pressures, particularly in inorganic compounds, *Proc. Amer. Acad. Arts Sci., 71*, 387–460, 1937.

Bridgman, P. W., *Studies in Large Plastic Flow and Fracture*, p. 13, McGraw-Hill, New York, 1952.

Chung, D. H., Elastic moduli of single-crystal and polycrystalline MgO, *Phil. Mag., 8*, 833, 1963.

Dandekar, D. P., Loss of shear strength in polycrystalline tungsten under shock compression, *J. Appl. Phys., 47*, 4703–4705, 1976.

Davies, G. F., Effective elastic moduli under hydrostatic stress, 1, Quasi-harmonic theory, *J. Phys. Chem. Solids, 35*, 1513, 1974.

Davies, G. F., and T. J. Ahrens, Measurements of elastic velocities of MgO under shock compression to 500 kilobars, *J. Geophys. Res., 78*, 7596, 1973.

Fowles, G. R., Attenuation of the shock wave produced in a solid by a flying plate, *J. Appl. Phys., 31*, 655, 1960.

Fowles, G. R., Shock wave compression of hardened and annealed 2024 aluminum, *J. Appl. Phys., 32*, 1475, 1961.

Grady, D. E., W. J. Murri, and P. S. DeCarli, Hugoniot sound velocities and phase transformations in two silicates, *J. Geophys. Res., 80*, 4857, 1975.

Kinsland, G. L., and W. A. Bassett, Strength of MgO polycrystals to combining pressures of 250 kbar at 25°C, *J. Appl. Phys., 48*, 978, 1977.

Paterson, M. S., and C. W. Weaver, Deformation of polycrystalline MgO under pressure, *J. Amer. Ceram. Soc., 53*, 463, 1970.

Ruoff, A. L., The linear shock particle velocity relationship, *J. Appl. Phys., 38*, 4976, 1967.

Spetzler, H., The effect of temperature and partial melting on velocity and attenuation in a simple binary system and effect of temperature and pressure on elastic properties of polycrystalline and single crystal MgO, 1 and 2, Ph.D. thesis, Calif. Inst. of Technol., Pasadena, 1971.

Spetzler, H., and D. L. Anderson, Discrepancies in elastic constant data for MgO polycrystals and single crystals, *J. Amer. Ceram. Soc., 54*, 520, 1971.

Thomsen, L., On the fourth order anharmonic equation of state of solids, *J. Phys. Chem. Solids, 31,* 2003, 1970.

Thomsen, L., The fourth order anharmonic theory: Elasticity and stability, *J. Phys. Chem. Solids, 33,* 363, 1972.

Van Thiel, M., L. B. Hord, W. H. Gust, A. C. Mitchell, M. D'Addario, K. Boutwell, E. Wilbarger, and B. Barret, Shock compression of deuterium to 900 kbar, *Phys. Earth Planet. Interiors, 9,* 57, 1974.

(Received August 20, 1976;
revised January 17, 1977;
accepted January 26, 1977.)